2017 13th IEEE International Conference on Control & Automation (ICCA)
July 3-6, 2017. Ohrid, Macedonia

Disturbance Observer-Based Saturated Control for a Quadrotor Landing on a Vessel*

Yanting Huang, Zewei Zheng, Liang Sun, and Bing Zhu

Abstract— **An autonomous vessel landing control algorithm of a quadrotor is investigated for the situation when the quadrotor hovers above the vessel with input saturation and disturbances. To facilitate the controller design, the problem of vessel landing is converted from general trajectory tracking problem of a quadrotor to a stabilization problem of relative motion. A fully actuated 4-DOF nonlinear relative altitude and attitude model with four control inputs is established. A nonlinear disturbance observer is developed to estimate the disturbances, while a compensation system is incorporated into the controller design to handle the input saturation. Then, a feedback controller is designed to synchronize the altitudes and attitudes of the quadrotor and the vessel. It is proved that the relative altitude and relative attitude converge to a small neighborhood of origin, and all states in the closed-loop system are uniformly ultimately bounded. Numerical simulation results demonstrate the effectiveness of the proposed controller.**

I. INTRODUCTION

With the development of the quadrotor helicopter, more and more considerable researches focused on its design, analysis, and operations have been performed. Compared with the conventional helicopters, quadrotor has many advantages including versatile maneuverability, hovering capacity and simple mechanical structure [1]–[3]. Therefore, it is used in several typical missions, such as search and rescue missions, surveillance, inspection, aerial cinematography [4]. Additionally, the application of quadrotor in open seas can provide the capability of efficient reconnaissance and survey on the ocean. This operation requires the quadrotor to complete the autonomous landing task on a vessel by means of its excellent operation capabilities. However, it is challenging to perform autonomous landing of a quadrotor on a vessel because pseudorandom ship motion caused by ship-wave interactions increases the difficulty of autonomous landing [5]. Besides, the time-varying disturbances from the airflow and the ocean currents are unpredictable [6]. All of these make the landing control problem particularly complicated.

A variety of methods have been applied to solve autonomous landing problem. In [6], the authors introduced an algorithm composed of the time-delay controller and the guidance law to avoid model uncertainties and unpredictable disturbances. The time-delay control is actively adopted to compensate for the model uncertainties of a rotorcraft while the guidance law considers crash avoidance, reentrance procedures and the effects of crosswind. Ref. [7] proposed a robust automatic landing system by using the H_∞ control, the dynamic inversion and the optimal observer compensating for wind shears and sensor errors. Moreover, based on the optimization of the steady landing condition, the generalized landing trajectory including position and attitude can be designed to guide the landing [8]. A tether is utilized to land a helicopter to shipdeck in [9], where two control modes are developed: position control mode and attitude-altitude control mode for achieving the task. Other landing methods include vision-guided landing methods [10]–[13], H_2/H_∞ [14] and pigeon-inspired optimization [15]. Furthermore, relative motion modeling method was generally used in spacecraft docking system to facilitate the controller design [16], [17]. Applications of relative motion modeling for landing a quadrotor on a vessel can convert the general trajectory tracking problem to a stabilization problem. However, the researches about this are comparatively limited.

Input saturation is common and inevitable in practical system. It may lead to severe performance degradation and even instability of the closed-loop system. Therefore, it should be considered in control design [18]. To compensate for the input saturation and the unknown disturbances, it's efficient to use the *disturbance observers*. A nonlinear disturbance observer is designed to deduce a signal disturbance term including unknown forces, torques and external disturbances, and then to compensate for the influence of the disturbances using proper feedback. Recently, the disturbance observer is widely applied to design controllers with strong robustness, such as control for trajectory tracking of wheeled mobile robots [19], fault estimation for a quadrotor [20], H_∞ control for nonlinear Markovian jump systems [21].

The whole vessel autonomous landing of a quadrotor is divided into two stages: the approaching phase and the landing phase. In the first stage, the quadrotor is approached to hover above the vessel by trajectory tracking control. In the second stage, the quadrotor selects appropriate time to descend vertically to the vessel. The disturbance including waves and sea surface wind and other airflow led to a complex landing environment for the landing phase, so the second stage is the key to the autonomous landing technology.

In this paper, we present a controller for autonomous landing of a quadrotor on a vessel using relative motion model which adapts to the situation when the quardrotor

*This work was supported by the National Natural Science Foundation of China (No.61503010), the Aeronautical Science Foundation of China (No.2016ZA51001), the China Postdoctoral Science Foundation (No.2016M590031), and the Fundamental Research Funds for the Central Universities (No.YWF-16-GJSYS-02).

The authors are with the Seventh Research Division, Science and Technology on Aircraft Control Laboratory, School of Automation Science and Electrical Engineering, Beihang University, Beijing, 100191 P.R. China huangyanting@buaa.edu.cn; zeweizheng@buaa.edu.cn; liangsun@buaa.edu.cn; zhubing@buaa.edu.cn

hovers above the vessel. The main contributions of this paper are summarized as: (1) A 4-DOF nonlinear relative motion model between a quadrotor and a vessel is established. (2) A disturbance observer-based backstepping technique is used to handle the problem of system couplings, asymmetric input saturation and uncertain disturbances. (3) Lyapunov stability analysis proves that all the states in the closed-loop system are uniformly ultimately bounded.

The structure of the paper is arranged as following. Problem statement is presented in Section II. It is devoted to design a disturbance observer and a controller in Section III. In Section IV, numerical simulations are performed to verify the proposed control approach, followed by conclusion in Section V.

II. PROBLEM STATEMENT

The relative motion of the quadrotor and the unmanned vessel is illustrated in Fig.1 [22]. As shown in Fig.1, the inertial frame and body-fixed frames of the quadrotor and the vessel are defined respectively. The inertial frame $E = \{O_e - x_e y_e z_e\}$ is fixed on the earth. The frame $B_1 = \{O_b^1 - x_b^1 y_b^1 z_b^1\}$ is taken as the body-fixed frame of the quadrotor, whose coordinate origin O_b^1 is the geometric center point of the quadrotor. Let $B_2 = \{O_b^2 - x_b^2 y_b^2 z_b^2\}$ denote the body-fixed frame of the unmanned vessel, whose coordinate defined similarly as B_1.

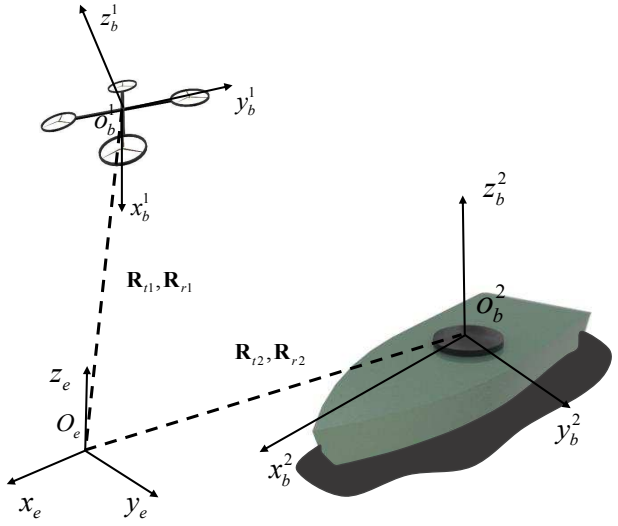

Fig. 1. Relative motion of the quadrotor and the vessel.

A. Models of the Quadrotor and the Unmanned Vessel

The presented controller in this paper is used for the situation when the quadrotor hovers above the unmanned vessel, so that we only consider the relative altitude and attitude between the quadrotor and unmanned vessel, controlling the position in Oxy plane is beyond the scope of this paper.

The kinematical equations of the quadrotor are governed by [23]:

$$\begin{cases} \dot{z}_1 = \boldsymbol{m}(\boldsymbol{\eta}_1)\boldsymbol{V}_1, \\ \dot{\boldsymbol{\eta}}_1 = \boldsymbol{R}_{r_1}\boldsymbol{\Omega}_1, \end{cases} \tag{1}$$

where z_1 and $\boldsymbol{\eta}_1 = [\phi_1, \theta_1, \psi_1]^T$ (consists of the roll angle ϕ_1, pitch angle θ_1, and yaw angle ψ_1) denote the altitude and attitude of quadrotor in E, respectively. $\boldsymbol{V}_1 = [u_1, v_1, w_1]^T$ and $\boldsymbol{\Omega}_1 = [p_1, q_1, r_1]^T$ are three translation velocities and three rotation velocities in B_1, respectively.

$$\boldsymbol{R}_{\boldsymbol{r_1}} = \frac{1}{C_{\theta_1}} \begin{bmatrix} C_{\theta_1} & S_{\phi_1}S_{\theta_1} & C_{\phi_1}S_{\theta_1} \\ 0 & C_{\phi_1}C_{\theta_1} & -S_{\phi_1}C_{\theta_1} \\ 0 & S_{\phi_1} & C_{\phi_1} \end{bmatrix}, \tag{2}$$

$\boldsymbol{m}(\boldsymbol{\eta_1}) = [-S_{\theta_1} \quad C_{\theta_1}S_{\phi_1} \quad C_{\theta_1}C_{\phi_1}]$ is the last row of the rotation matrix from B_1 to E, where $S_{(\cdot)} \triangleq \sin(\cdot)$, $C_{(\cdot)} \triangleq \cos(\cdot)$. In addition, we have $\dot{\boldsymbol{m}}(\boldsymbol{\eta}_1) = \boldsymbol{m}(\boldsymbol{\eta}_1)\boldsymbol{S}(\boldsymbol{\Omega}_1)$, where $\boldsymbol{S}(\boldsymbol{\Omega}_1)$ is the skew-symmetric matrix defined as

$$\boldsymbol{S}(\boldsymbol{\Omega}_1) = \begin{bmatrix} 0 & -r_1 & q_1 \\ r_1 & 0 & -p_1 \\ -q_1 & p_1 & 0 \end{bmatrix}.$$

The dynamic equations of the quadrotor can be expressed by [23]

$$\begin{cases} m_1\dot{\boldsymbol{V}}_1 + \boldsymbol{S}(\boldsymbol{\Omega}_1)m_1\boldsymbol{V}_1 = \boldsymbol{F} - \boldsymbol{F}_{aero} - \boldsymbol{F}_{grav} + \boldsymbol{d}_f, \\ \boldsymbol{I}_1\dot{\boldsymbol{\Omega}}_1 + \boldsymbol{S}(\boldsymbol{\Omega}_1)\boldsymbol{I}_1\boldsymbol{\Omega}_1 = \boldsymbol{T} - \boldsymbol{T}_{aero} + \boldsymbol{d}_m, \end{cases} \tag{3}$$

where m_1 denotes the mass of the quadrotor, $\boldsymbol{I_1} = \text{diag}\{I_x, I_y, I_z\}$ is the total inertial matrix of the quadrotor. $\boldsymbol{F} = [0, 0, F_{total}]^T$ and $\boldsymbol{T} = [M_x, M_y, M_z]^T$ are respectively propeller thrust and torque of the quadrotor, with $F_{total} = \sum_{i=1}^{4} F_i$, $M_x = d(F_2 - F_4)$, $M_y = d(F_3 - F_1)$, $M_z = c\sum_{i=1}^{4}(-1)^{i+1}F_i$. The forces $F_i (i = 1, 2, 3, 4)$ are the thrusts generated by the muti propellers, $d \in \mathbb{R}$ is the distance from the rotor axes to the epicenter of the quadrotor and $c > 0$ is the drag factor. $\boldsymbol{F}_{aero}$, $\boldsymbol{F}_{grav}$ and $\boldsymbol{T}_{aero}$ are aerodynamic force, gravity and aerodynamic torques, which are described as $\boldsymbol{F}_{aero} = \boldsymbol{K}_t\boldsymbol{V}_1$, $\boldsymbol{F}_{grav} = m_1\boldsymbol{R}_{t_1}^T\boldsymbol{g}$, $\boldsymbol{T}_{aero} = \boldsymbol{K}_r\boldsymbol{\Omega}_1$, respectively, where $\boldsymbol{K}_t = \text{diag}\{K_{t1}, K_{t2}, K_{t3}\}$ and $\boldsymbol{K}_r = \text{diag}\{K_{r1}, K_{r2}, K_{r3}\}$ are aerodynamic friction matrices, $\boldsymbol{R}_{t_1}$ is the rotation matrix from B_1 to E, $\boldsymbol{g} = [0, 0, g_s]^T (g_s = 9.8m/s)$ is the gravity vector. $\boldsymbol{d}_f = [d_{fx}, d_{fy}, d_{fz}]^T$ and $\boldsymbol{d}_m = [d_{mx}, d_{my}, d_{mz}]^T$ include the aerodynamic effects and external disturbances.

From (1) and (3), the second-order derivative of altitude z_1 with respect to time gives

$$\ddot{z}_1 = \frac{n(\boldsymbol{\eta}_1)F_{total} - \boldsymbol{m}(\boldsymbol{\eta}_1)\boldsymbol{K}_t\boldsymbol{V}_1 + \boldsymbol{m}(\boldsymbol{\eta}_1)\boldsymbol{d}_f}{m_1} - g_s, \tag{4}$$

where $n(\boldsymbol{\eta}_1) = C_{\theta_1}C_{\phi_1}$ is the last element of $\boldsymbol{m}(\boldsymbol{\eta}_1)$.

Similar with the model of quadrotor, the 4-DOF kinematical model of the unmanned vessel can be expressed as [24]

$$\begin{cases} \dot{z}_2 = \boldsymbol{J}(\boldsymbol{\eta}_2)\boldsymbol{V}_2, \\ \dot{\boldsymbol{\eta}}_2 = \boldsymbol{R}_{r_2}\boldsymbol{\Omega}_2, \end{cases} \tag{5}$$

where z_2 and $\boldsymbol{\eta}_2 = [\phi_2, \theta_2, \psi_2]^T$ are the altitude and attitude of the unmanned vessel in E, respectively. $\boldsymbol{V}_2 = [u_2, v_2, w_2]^T$ and $\boldsymbol{\Omega}_2 = [p_2, q_2, r_2]^T$ are the velocity and the angular velocity of the unmanned vessel defined in B_2,

respectively. $\boldsymbol{J}(\boldsymbol{\eta}_2) = [-S_{\theta_2}\ C_{\theta_2}S_{\phi_2}\ C_{\theta_2}C_{\phi_2}]$ is the last row of the rotation matrix from B_2 to E. $\boldsymbol{R}_{r_2}$ is defined as

$$\boldsymbol{R_{r_2}} = \frac{1}{C_{\theta_2}} \begin{bmatrix} C_{\theta_2} & S_{\phi_2}S_{\theta_2} & C_{\phi_2}S_{\theta_2} \\ 0 & C_{\phi_2}C_{\theta_2} & -S_{\phi_2}C_{\theta_2} \\ 0 & S_{\phi_2} & C_{\phi_2} \end{bmatrix}.$$

In general, the unmanned vessel is designed to have sufficient longitudinal and transverse metacentric height to stabilize the rolling and pitching motions of the vessel. In this case, we can neglect the vessel's montions in pitch and roll, scilicet variables ϕ_2, θ_2, p_2, q_2 are always zero. So $\boldsymbol{J}(\boldsymbol{\eta}_2)$ and $\boldsymbol{R}_{r2}$ are simplified as $\boldsymbol{J}^{'}(\boldsymbol{\eta}_2) = [0\ 0\ 1]$, $\boldsymbol{R}_{r_2}^{'} = \boldsymbol{I}$, where $\boldsymbol{I}$ is a unit matrix.

The dynamic equations of the vessel can be obtained as [24]

$$\begin{cases} \boldsymbol{M}_1\dot{\boldsymbol{V}}_2 = -\boldsymbol{C}_1(\boldsymbol{V}_2)\boldsymbol{V}_2 - \boldsymbol{D}_1\boldsymbol{V}_2 + \boldsymbol{\Gamma}_1 + \boldsymbol{d}_{tf}, \\ \boldsymbol{M}_2\dot{\boldsymbol{\Omega}}_2 = -\boldsymbol{C}_2(\boldsymbol{\Omega}_2)\boldsymbol{\Omega}_2 - \boldsymbol{D}_2\boldsymbol{\Omega}_2 + \boldsymbol{\Gamma}_2 + \boldsymbol{d}_{tm}, \end{cases} \tag{6}$$

where $\boldsymbol{M}_1 = \text{diag}\{m_{11}, m_{22}, m_{33}\}$ and $\boldsymbol{M}_2 = \text{diag}\{0, 0, m_{44}\}$ are nonsingular and positive definite inertia matrices. $\boldsymbol{D}_1$=diag$\{d_{11}, d_{22}, d_{33}\}$ and $\boldsymbol{D}_2$=diag$\{0, 0, d_{44}\}$ are the damping matrices. $\boldsymbol{\Gamma}_1$=$[\tau_x, \tau_y, 0]^T$ and $\boldsymbol{\Gamma}_2$=$[0, 0, \tau_z]^T$ are the system control inputs. $\boldsymbol{C}_1(\boldsymbol{V}_2)$ and $\boldsymbol{C}_2(\boldsymbol{\Omega}_2)$ are given as

$$\boldsymbol{C}_1 = \begin{bmatrix} 0 & 0 & -m_{22}v_2 \\ 0 & 0 & m_{11}u_2 \\ 0 & 0 & 0 \end{bmatrix}, \boldsymbol{C}_2 = \begin{bmatrix} 0 & 0 & 0 \\ 0 & 0 & 0 \\ m_{22}v_2 & -m_{11}u_2 & 0 \end{bmatrix}.$$

$\boldsymbol{d}_{tf} = [d_{t1}, d_{t2}, d_{t3}]^T$ and $\boldsymbol{d}_{tm} = [0, 0, d_{t4}]^T$ include the unmodeled dynamics and the unknown bounded time-varying disturbances from the environment.

B. 4-DOF Relative Motion Model

According to the models proposed in the above subsection, the relative kinematic equations are presented as

$$\begin{cases} \dot{z}_e = \boldsymbol{m}(\boldsymbol{\eta_1})\boldsymbol{V_1} - w_2, \\ \dot{\boldsymbol{\eta}}_e = \boldsymbol{R_{r_1}}\boldsymbol{\Omega_e}, \end{cases} \tag{7}$$

where $z_e = z_1 - z_2$ and $\boldsymbol{\eta}_e = \boldsymbol{\eta}_1 - \boldsymbol{\eta}_2 = [\phi_e, \theta_e, \psi_e]^T$ is the relative altitude and attitude in E, respectively. $\boldsymbol{\Omega}_e = \boldsymbol{\Omega}_1 - \boldsymbol{R}_{r_{12}}\boldsymbol{\Omega}_2 = [p_e, q_e, r_e]^T$ is the relative angular velocity in B_1. $\boldsymbol{\Omega}_2 = [0, 0, r_2]^T$ and $\boldsymbol{R}_{r_{12}} = \boldsymbol{R}_{r_1}^{-1}\boldsymbol{R}_{r_2}^{'} = \boldsymbol{R}_{r_1}^{-1}$ is rotation matrix from B_2 to B_1.

Similar with the simplified form of the relative kinematics, the relative dynamics can be expressed as

$$\begin{cases} \ddot{z}_e = \ddot{z}_1 - \ddot{z}_2 = f_1 + U_1 + d_1, \\ \dot{\boldsymbol{\Omega}}_e = \boldsymbol{f}_2 + \boldsymbol{U}_2 + \boldsymbol{d}_2, \end{cases} \tag{8}$$

where $f_1 = -\frac{\boldsymbol{m}(\boldsymbol{\eta}_1)\boldsymbol{K}_t\boldsymbol{V}_1}{m_1} + \frac{d_{33}}{m_{33}}w_2 - g_s$. $U_1 = \frac{n(\boldsymbol{\eta}_1)F_{total}}{m_1}$. $d_1 = \frac{\boldsymbol{m}(\boldsymbol{\eta}_1)\boldsymbol{d}_f}{m_1} - \frac{d_{t3}}{m_{33}}$.

$$\boldsymbol{f}_2 = \begin{bmatrix} \frac{-K_{r_1}p_1}{I_x} \\ \frac{-K_{r_2}q_1}{I_y} \\ \frac{-K_{r_3}r_1}{I_z} \end{bmatrix} - \begin{bmatrix} \frac{(I_z-I_y)q_1r_1}{I_x} \\ \frac{(I_x-I_z)p_1r_1}{I_y} \\ \frac{(I_y-I_x)p_1q_1}{I_z} \end{bmatrix} - \boldsymbol{R}_{r_{12}}\begin{bmatrix} 0 \\ 0 \\ r_2^{'} \end{bmatrix} - \dot{\boldsymbol{R}}_{r_{12}}\begin{bmatrix} 0 \\ 0 \\ r_2 \end{bmatrix},$$

with $r_2^{'} = \frac{\tau_z - d_{44}r_2 + (m_{11}-m_{22})u_2v_2}{m_{44}}$; $\boldsymbol{U}_2 = [\frac{M_x}{I_x}, \frac{M_y}{I_y}, \frac{M_z}{I_z}]^T$; $\boldsymbol{d}_2 = [\frac{d_{mx}}{I_x}, \frac{d_{my}}{I_y}, \frac{d_{mz}}{I_z}]^T - \boldsymbol{R}_{r_{12}}[0, 0, \frac{d_{t4}}{m_{44}}]^T$.

With denoting the system states $\boldsymbol{e}_1 = [z_e, \boldsymbol{\eta}_e^T]^T$ and $\boldsymbol{e}_2 = [\dot{z}_e, \boldsymbol{\Omega}_e^T]^T$, then the relative motion model (7) and (8) can be rewritten as

$$\begin{cases} \dot{\boldsymbol{e}}_1 = \boldsymbol{n}, \\ \dot{\boldsymbol{e}}_2 = \boldsymbol{f} + \boldsymbol{U} + \boldsymbol{d}, \end{cases} \tag{9}$$

where $\boldsymbol{n} = [\boldsymbol{m}(\boldsymbol{\eta_1})\boldsymbol{V}_1 - w_2, (\boldsymbol{R}_{r_1}\boldsymbol{\Omega}_e)^T]^T$, $\boldsymbol{f} = [f_1, \boldsymbol{f}_2^T]^T$, $\boldsymbol{u} = [U_1, \boldsymbol{U}_2^T]^T$ and $\boldsymbol{d} = [d_1, \boldsymbol{d}_2^T]^T$.

C. Control Objective

Consider that the quadrotor's control input $\boldsymbol{U} = [U_1, U_2, U_3, U_4]^T$ is subject to the following constraints

$$-U_i^- \le U_i \le U_i^+, i = 1, 2, 3, 4$$

where $-U_i^-$ and $-U_i^+$ are the known lower and upper bounds of input saturation constraints. Thus, the control input $\boldsymbol{U}$ can be constructed as

$$U_i = \begin{cases} U_i^+ & if\ U_{0i} > U_i^+ \\ U_{0i} & if\ -U_i^- \le U_{0i} \le U_i^+ \\ U_i^- & if\ U_{0i} < -U_i^- \end{cases} \tag{10}$$

where $\boldsymbol{U_0} = [U_{01}, U_{02}, U_{03}, U_{04}]^T$ is the control input to be designed in the presence of input saturation. To facilitate the controller design later, define $\Delta\boldsymbol{U} = \boldsymbol{U} - \boldsymbol{U_0}$. Then, the model (9) changes to

$$\begin{cases} \dot{\boldsymbol{e}}_1 = \boldsymbol{n}, \\ \dot{\boldsymbol{e}}_2 = \boldsymbol{f} + \boldsymbol{U}_0 + \boldsymbol{D}, \end{cases} \tag{11}$$

with the system lumped disturbance

$$\boldsymbol{D} = \Delta\boldsymbol{U} + \boldsymbol{d}. \tag{12}$$

For the subsequent developement of control laws, the following assumptions are made.

Assumption 1: The quadrotor and the vessel are rigid bodies, and the quadrotor is symmetrical with respect to the axes $O_b^1x_b^1$,$O_b^1y_b^1$,$O_b^1z_b^1$.

Assumption 2: The initial position of the quadrotor before the action of designed controller is above the unmanned vessel, and the pitch angle of the quadrotor is bounded as $\theta_1 \in (-\frac{\pi}{2}, \frac{\pi}{2})$.

Assumption 3: The unknown external disturbances $\boldsymbol{d}_f$, $\boldsymbol{d}_m$ and $\boldsymbol{d}_t$ are continuous and bounded, and their derivatives are also bounded. All states of the unmanned vessel are bounded under the effect of the vessel's input.

The control objective is to design feedback control law $\boldsymbol{U}_0$ in (11) with input saturation such that the quadrotor can land on the vessel steadily, that is, tracking error of $\boldsymbol{e}_1$ (consists of relative altitude z_e and relative attitude $\boldsymbol{\eta}_e$) is restricted to small values, while it is guaranteed that all signals of the resulting closed-loop system remain bounded.

III. CONTROL DESIGN AND STABILITY ANALYSIS

A. Disturbance Observer Design

In the process of a quadrotor landing on an unmanned vessel, directly measuring the disturbances is very difficult. However, the disturbance observer technique provides an alternative approach. Applying the exponential convergent observer for a general nonlinear system from [25], we construct the nonlinear disturbance observer for the lumped disturbance vector $\boldsymbol{D}$ in (11) as

$$\begin{cases} \dot{\boldsymbol{z}} = -\boldsymbol{L}\boldsymbol{z} - \boldsymbol{L}(\boldsymbol{L}\boldsymbol{e}_2 + \boldsymbol{f} + \boldsymbol{U}_0), \\ \widehat{\boldsymbol{D}} = \boldsymbol{z} + \boldsymbol{L}\boldsymbol{e}_2, \end{cases} \tag{13}$$

where $\widehat{\boldsymbol{D}}$ is the estimate of $\boldsymbol{D}$, $\boldsymbol{z}$ is the state vector of the disturbance observer, and $\boldsymbol{L} \in \mathbb{R}^{4\times4}$ is a positive definite diagonal gain matrix for observer.

Define the observation error $\widetilde{\boldsymbol{D}}$ of $\boldsymbol{D}$ as $\widetilde{\boldsymbol{D}} = \boldsymbol{D} - \widehat{\boldsymbol{D}}$. From (11) and (13), we have

$$\begin{aligned} \dot{\widetilde{\boldsymbol{D}}} &= \dot{\boldsymbol{z}} + \boldsymbol{L}\dot{\boldsymbol{e}}_2 \\ &= -\boldsymbol{L}\boldsymbol{z} - \boldsymbol{L}(\boldsymbol{L}\boldsymbol{e}_2 + \boldsymbol{f} + \boldsymbol{u}_0) + \boldsymbol{L}(\boldsymbol{f} + \boldsymbol{u}_0 + \boldsymbol{D}) \\ &= -\boldsymbol{L}\boldsymbol{z} - \boldsymbol{L}(\boldsymbol{L}\boldsymbol{e}_2 + \boldsymbol{D}) \\ &= \boldsymbol{L}(\boldsymbol{D} - \widehat{\boldsymbol{D}}). \end{aligned} \tag{14}$$

Then, the time derivative of $\widetilde{\boldsymbol{D}}$ is

$$\dot{\widetilde{\boldsymbol{D}}} = \dot{\boldsymbol{D}} - \boldsymbol{L}(\boldsymbol{D} - \widehat{\boldsymbol{D}}) = \dot{\boldsymbol{D}} - \boldsymbol{L}\widetilde{\boldsymbol{D}}. \tag{15}$$

If the lumped disturbance vector $\boldsymbol{D}$ in (11) satisfies $\| \dot{\boldsymbol{D}} \| \leq \epsilon$ with a positive scalar ϵ, then the disturbance observer (13) guarantees that disturbance observation error $\widetilde{\boldsymbol{D}}$ is always bounded. These will be demonstrated in stability analysis.

B. Backstepping Controller Design

In this subsection, we present the controller that achieves the control objective as stated in Section II, assuming that states of the quadrotor and the vessel are all measurable.

Define the error vectors as

$$\boldsymbol{z}_1 = \boldsymbol{e}_1 - \boldsymbol{e}_{1d} \tag{16}$$

$$\boldsymbol{z}_2 = \boldsymbol{e}_2 - \boldsymbol{\alpha} \tag{17}$$

where $\boldsymbol{e}_{1d} = [z_{ed}, \boldsymbol{\eta}_{ed}^T]^T$ is the desired value, $\boldsymbol{\alpha}$ is a virtual control to be designed later. The control law design consists of two steps.

Step 1: Denote the Lyapunov function candidate as:

$$V_1 = \frac{1}{2}\boldsymbol{z}_1^T\boldsymbol{z}_1 \tag{18}$$

Since the time derivative of $\boldsymbol{e}_1$ is given as

$$\dot{\boldsymbol{e}}_1 = \begin{bmatrix} \dot{z}_e \\ \dot{\boldsymbol{\eta}}_e \end{bmatrix} = \begin{bmatrix} \dot{z}_e \\ \boldsymbol{R}_{r1}\boldsymbol{\Omega}_e \end{bmatrix} = \begin{bmatrix} 1 & 0 \\ 0 & \boldsymbol{R}_{r1} \end{bmatrix} \begin{bmatrix} \dot{z}_e \\ \boldsymbol{\Omega}_e \end{bmatrix} = \boldsymbol{R}\boldsymbol{e}_2 \tag{19}$$

where $\boldsymbol{R} = \mathrm{diag}\{1, \boldsymbol{R}_{r1}\}$. Then we calculate the time derivative of $\boldsymbol{z}_1$ as

$$\dot{\boldsymbol{z}}_1 = \dot{\boldsymbol{e}}_1 - \dot{\boldsymbol{e}}_{1d} = \boldsymbol{R}(\boldsymbol{z}_2 + \boldsymbol{\alpha}) - \dot{\boldsymbol{e}}_{1d} \tag{20}$$

The derivative of V_1 along the solution of (20) is

$$\dot{V}_1 = \boldsymbol{z}_1^T\dot{\boldsymbol{z}}_1 = \boldsymbol{z}_1^T(\boldsymbol{R}\boldsymbol{\alpha} - \dot{\boldsymbol{e}}_{1d}) + \boldsymbol{z}_1^T\boldsymbol{R}\boldsymbol{z}_2 \tag{21}$$

Design the virtual control

$$\boldsymbol{\alpha} = \boldsymbol{R}^{-1}(-\boldsymbol{k}_1\boldsymbol{z}_1 + \dot{\boldsymbol{e}}_{1d}) \tag{22}$$

where $\boldsymbol{k}_1 \in \mathbb{R}^{4\times4}$ is a positive-definite symmetric matrix. Substituting (22) into (21) yields

$$\dot{V}_1 = -\boldsymbol{z}_1^T\boldsymbol{k}_1\boldsymbol{z}_1 + \boldsymbol{z}_1^T\boldsymbol{R}\boldsymbol{z}_2 \tag{23}$$

The crossing term $\boldsymbol{z}_1^T\boldsymbol{R}\boldsymbol{z}_2$ will be cancelled in the next step.

Step 2: Consider the Lyapunov function as:

$$V_2 = V_1 + \frac{1}{2}\boldsymbol{z}_2^T\boldsymbol{z}_2 + \frac{1}{2}\widetilde{\boldsymbol{D}}^T\widetilde{\boldsymbol{D}} \tag{24}$$

Then the time derivative of V_2 is

$$\begin{aligned} \dot{V}_2 &= \dot{V}_1 + \boldsymbol{z}_2^T\dot{\boldsymbol{z}}_2 + \widetilde{\boldsymbol{D}}^T\dot{\widetilde{\boldsymbol{D}}} \\ &= \dot{V}_1 + \boldsymbol{z}_2^T(\boldsymbol{f} + \boldsymbol{U}_0 + \boldsymbol{D} - \dot{\boldsymbol{\alpha}}) + \widetilde{\boldsymbol{D}}^T\dot{\widetilde{\boldsymbol{D}}} \end{aligned} \tag{25}$$

Therefore, based on the observation of disturbance, control input command for system model (11) can be designed as

$$\boldsymbol{U}_0 = -\boldsymbol{k}_2\boldsymbol{z}_2 - \boldsymbol{R}^T\boldsymbol{z}_1 + \dot{\boldsymbol{\alpha}} - \boldsymbol{f} - \widehat{\boldsymbol{D}} \tag{26}$$

where $\boldsymbol{k}_2 \in \mathbb{R}^{4\times4}$ is a positive-definite symmetric matrix,

$$\dot{\boldsymbol{\alpha}} = \dot{\boldsymbol{R}}^{-1}(-\boldsymbol{k}_1\boldsymbol{z}_1 + \dot{\boldsymbol{e}}_{1d}) + \boldsymbol{R}^{-1}[-\boldsymbol{k}_1(\dot{\boldsymbol{e}}_1 - \dot{\boldsymbol{e}}_{1d}) + \ddot{\boldsymbol{e}}_{1d}] \tag{27}$$

Substituting (26) into (25) yields

$$\begin{aligned} \dot{V}_2 &= \dot{V}_1 - \boldsymbol{z}_2^T\boldsymbol{k}_2\boldsymbol{z}_2 - \boldsymbol{z}_2^T\boldsymbol{R}\boldsymbol{z}_1 + \widetilde{\boldsymbol{D}}^T\dot{\widetilde{\boldsymbol{D}}} \\ &= -\boldsymbol{z}_1^T\boldsymbol{k}_1\boldsymbol{z}_1 - \boldsymbol{z}_2^T\boldsymbol{k}_2\boldsymbol{z}_2 + \widetilde{\boldsymbol{D}}^T(\dot{\boldsymbol{D}} - \boldsymbol{L}\widetilde{\boldsymbol{D}}) \end{aligned} \tag{28}$$

Then we can derive the stability results in following theorem.

Theorem 1: Under Assumptions 1-3, consider the closed-loop system consisting of the relative model (11), the controller designed by (26) with disturbance observer (13). There exists appropriate design parameters $\lambda_m(\boldsymbol{L}) \geq \frac{1}{2}, \lambda_m(\boldsymbol{k}_i) \geq 0 (i = 1, 2)$ such that all states in the closed-loop control system remain uniformly ultimately bounded and the relative tracking errors $\boldsymbol{z_1}$ and $\boldsymbol{z_2}$ converge to a small neighborhood of zero, where $\lambda_m(\cdot)$ represents the minimum eigenvalue of a matrix.

Proof: Considering the Lyapunov function candidate as

$$V_2 = \frac{1}{2}\boldsymbol{z}_1^T\boldsymbol{z}_1 + \frac{1}{2}\boldsymbol{z}_2^T\boldsymbol{z}_2 + \frac{1}{2}\widetilde{\boldsymbol{D}}^T\widetilde{\boldsymbol{D}} \geq 0$$

Applying $\| \dot{\boldsymbol{D}} \| \leq \epsilon$ and Young inequality [25], we can obtain the time derivative of V_2 as

$$\begin{aligned} \dot{V}_2 &= -\boldsymbol{z}_1^T\boldsymbol{k}_1\boldsymbol{z}_1 - \boldsymbol{z}_2^T\boldsymbol{k}_2\boldsymbol{z}_2 - \widetilde{\boldsymbol{D}}^T\boldsymbol{L}\widetilde{\boldsymbol{D}} + \widetilde{\boldsymbol{D}}^T\dot{\boldsymbol{D}} \\ &\leq -\boldsymbol{z}_1^T\boldsymbol{k}_1\boldsymbol{z}_1 - \boldsymbol{z}_2^T\boldsymbol{k}_2\boldsymbol{z}_2 - \widetilde{\boldsymbol{D}}^T(\boldsymbol{L} - \frac{1}{2}\boldsymbol{I})\widetilde{\boldsymbol{D}} + \frac{1}{2}\epsilon^2 \end{aligned} \tag{29}$$

when $\lambda_m(\boldsymbol{L}) \geq \frac{1}{2}, \lambda_m(\boldsymbol{k}_i) \geq 0 (i = 1, 2)$,

$$\dot{V}_2 \leq -2\lambda_s V_2 + \frac{1}{2}\epsilon^2 \tag{30}$$

where $\lambda_s = \min\{\lambda_m(\boldsymbol{k}_1), \lambda_m(\boldsymbol{k}_2), \lambda_m(\boldsymbol{L})-\frac{1}{2}\}$. Solving (30) by applying comparison principle [26], we derive

$$V_2 \leq \left[V_2(0) - \frac{\epsilon^2}{4\lambda_s}\right] e^{-2\lambda_s t} + \frac{\epsilon^2}{4\lambda_s} \tag{31}$$

From the definition of V_2, we have

$$\| \boldsymbol{x} \| \leq \sqrt{[2V_2(0) - \frac{\epsilon^2}{2\lambda_s}]e^{-2\lambda_s t} + \frac{\epsilon^2}{2\lambda_s}} \tag{32}$$

where $\boldsymbol{x} = [\boldsymbol{z}_1^T, \boldsymbol{z}_2^T, \widetilde{\boldsymbol{D}}^T]^T$. It implies that the state $\boldsymbol{x}$ will coverage eventually to the set $\Omega_x = \{\boldsymbol{x} : \| \boldsymbol{x} \| \leq \frac{\epsilon}{\sqrt{2\lambda_s}}\}$, whose size can be determined by the parameter ϵ. Therefore, $\boldsymbol{z}_1$, $\boldsymbol{z}_2$, and $\widetilde{\boldsymbol{D}}$ are uniformly ultimately bounded. From (16),(17),(22), and (26), the facts of $\boldsymbol{z}_1$, $\boldsymbol{z}_2$ are bounded and Assumption 3, the states $\boldsymbol{e}_1$, $\boldsymbol{e}_2$ and the control input command $\boldsymbol{U}_0$ are hence all bounded, so that z_1 and $\boldsymbol{\eta}_1$ are bounded. Thus, the proposed controller can guarantee the boundedness of all states in the close-loop system.

IV. NUMERICAL SIMULATIONS

In this section, to verify the effectiveness of the proposed autonomous landing approach, a simulation is carried out. The controller is designed for the situation when the quadrotor hovers above the vessel, so the initial conditions are selected as $z_1(0) = 0.5(\text{m})$, $\boldsymbol{\eta}_1(0) = [-9.7, 9.7, 0]^T(\text{deg})$, $\boldsymbol{\Omega}_1(0) = [5.73, 5.73, 5.73]^T(\text{deg/s})$, $\boldsymbol{V}_1(0) = [0.1, 0.1, 0.1]^T(\text{m/s})$, $z_2(0) = 0(\text{m})$, $\boldsymbol{\eta}_2(0) = [0, 0, 2]^T(\text{rad})$, $\boldsymbol{V}_2(0) = [0.01, 0, 0]^T(\text{m/s})$, $\boldsymbol{\Omega}_2(0) = [0, 0, 0]^T(\text{rad/s})$ The inertial, geometric, aerodynamic, hydrodynamic parameters of quadrotor and vessel are $m_1 = 2(\text{kg})$, $I_x = I_y = 1.2416(\text{Nm}\cdot\text{s}^2/\text{rad})$, $I_z = 2.4832(\text{Nm}\cdot\text{s}^2/\text{rad})$, $K_{t1} = K_{t2} = K_{t3} = 0.01(\text{N}\cdot\text{s/m})$, $K_{r1} = K_{r2} = K_{r3} = 0.001(\text{N}\cdot\text{s/rad})$, $m_{11} = 200(\text{kg})$, $m_{22} = 250(\text{kg})$, $m_{33} = 90(\text{kg})$, $m_{44} = 80(\text{kg})$, $d_{11} = 70(\text{kg})$, $d_{22} = 100(\text{kg})$, $d_{33} = 60(\text{kg})$, $d_{44} = 50(\text{kg})$. The inputs of the vessel are set as $\boldsymbol{\Gamma}_1$=$[15, 10, 0]^T(\text{N})$ and $\boldsymbol{\Gamma}_2$=$[0, 0, 5]^T(\text{Nm})$.

The magnitude of the quadrotor's actuated control inputs are specified in the range of $U_1 \in [0, 10](\text{N})$, $U_2 \in [-2, 6](\text{Nm})$, $U_3 \in [-2, 6](\text{Nm})$, $U_4 \in [-6, 6](\text{Nm})$. External disturbances are specified as [27] [28]

$$\boldsymbol{d}_{tf} = \begin{bmatrix} \alpha_1 {u_2}^{\beta_1} \\ \alpha_2 \text{sgn}(v_2)|v_2|^{\beta_2} \\ -1.5\text{sin}(0.05t) \end{bmatrix}, \boldsymbol{d}_{tm} = \begin{bmatrix} 0 \\ 0 \\ \alpha_3 \text{sgn}(r_2)|r_2|^{\beta_3} \end{bmatrix},$$

$$\boldsymbol{d}_f = \begin{bmatrix} 0.06 - 0.04\text{sin}(\omega_0 t) + 0.05\text{cos}(\omega_0 t) \\ 0.07 + 0.05\text{sin}(\omega_0 t) - 0.04\text{cos}(\omega_0 t) \\ 0.04 - 0.03\text{sin}(\omega_0 t) + 0.03\text{cos}(\omega_0 t) \end{bmatrix} + \boldsymbol{\zeta}_1,$$

$$\boldsymbol{d}_m = \begin{bmatrix} d_1 + d_2|p_1| & 0 & 0 \\ 0 & d_3 + d_4|q_1| & 0 \\ 0 & 0 & d_5 + d_6|r_1| \end{bmatrix} \begin{bmatrix} p_1 \\ q_1 \\ r_1 \end{bmatrix} + \boldsymbol{\zeta}_2,$$

where $\alpha_1 = 2.44$, $\alpha_2 = 13.0$, $\alpha_3 = 0.5$, $\beta_1 = 1.51$, $\beta_2 = 1.75$, $\beta_3 = 1.59$, $\omega_0 = 0.02$, $d_i (i = 1, 2, 3, 4, 5, 6)$ are the damping coefficients chosen as $[d_1, d_2, d_3, d_4, d_5, d_6]^T = [0.1, 0.15, 0.1, 0.15, 0.1, 0.15]^T$, $\boldsymbol{\zeta}_1$ and $\boldsymbol{\zeta}_2$ are normally distributed noise signals with zero mean and variance of 0.01. Additionally, The controller and observer gains are set as $\boldsymbol{k}_1 = [0.01, 0.1, 1, 2]^T$, $\boldsymbol{k}_2 = [1, 3.5, 6.5, 6.5]^T$, $\boldsymbol{L} = 0.3\boldsymbol{I}_4$.

The simulation results of proposed control law are shown in Figs.2-5. As shown in Fig.2, the relative altitude and attitude between the quadrotor and vessel tend to zero. That is, the quadrotor can track the altitude and attitude of the unmanned vessel with a high precision. Fig.3 shows that the velocity of the quadrotor can track the respective vessel's values. Fig.4 describes control inputs of the quadrotor. It can be seen that control inputs with input constraints are limited before putting them on the actual actuators. Fig.5 shows that the estimation error of disturbances is bounded. The simulation result demonstrates that the proposed controller and disturbance observer are capable of attaining satisfactory autonomous landing performance.

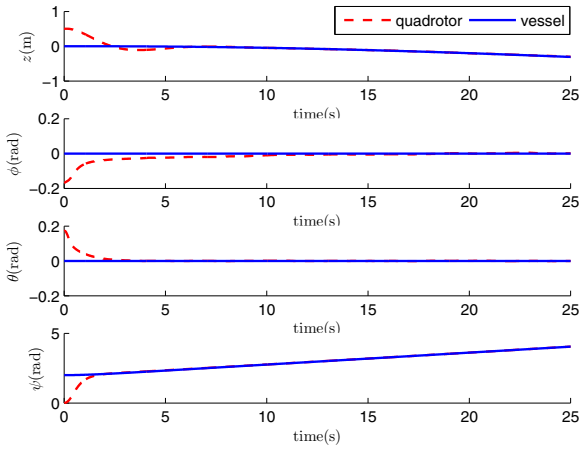

Fig. 2. Altitude and attitude of the quadrotor and vessel.

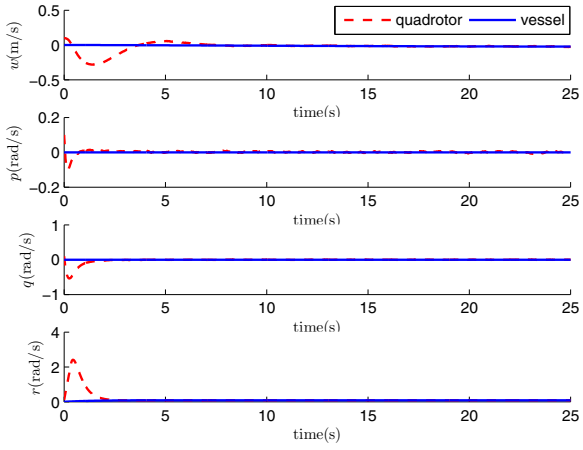

Fig. 3. Velocity of the quadrotor and vessel.

V. CONCLUSIONS

In this paper, we devote to solving the autonomous vessel landing problem for the situation when the quadrotor hovers

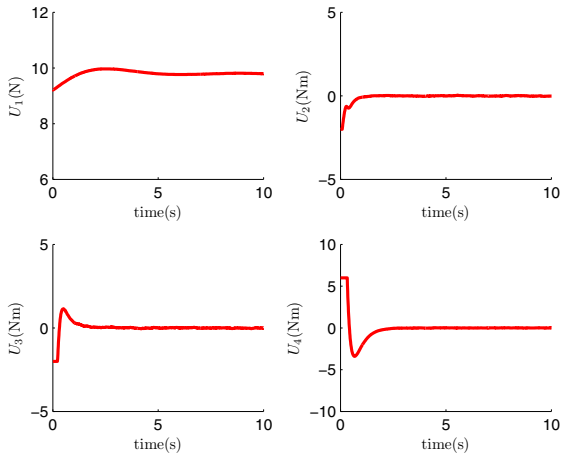

Fig. 4. control inputs of the quadrotor.

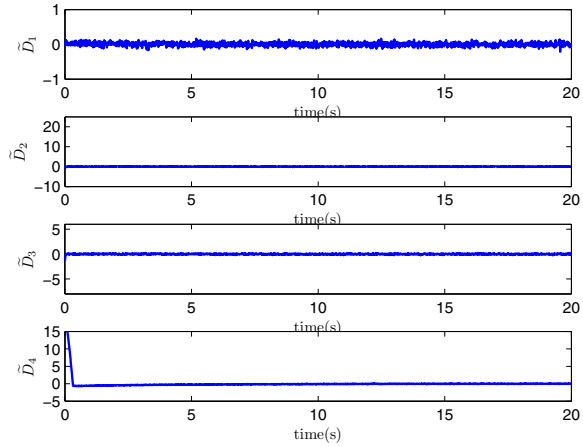

Fig. 5. Lumped disturbance observation errors.

above the vessel considering input saturation and disturbances. A fully actuated 4-DOF nonlinear relative motion model with four control inputs is established. The proposed controller is designed in the framework of backstepping with a nonlinear disturbance observer added to estimate the disturbances, while the input saturation can be handled by a compensation system simultaneously. Stability analysis implies that the tracking errors of relative altitude and relative attitude are uniformly ultimately bounded. The effectiveness of the proposed control approach is verified by simulations.

REFERENCES

[1] Z. Zuo and P. Ru, "Augmented L1 adaptive tracking control of quad-rotor unmanned aircrafts," *IEEE Transactions on Aerospace & Electronic Systems*, vol. 50, no. 4, pp. 3090-3101, 2014.

[2] Z. Zuo, "Trajectory tracking control design with command-filtered compensation for a quadrotor," *IET Control Theory & Applications*, vol. 19, no. 11, pp. 2343-2355, 2010.

[3] S. Islam, P. X. Liu and A. El Saddik, "Robust control offour-rotor unmanned aerial vehicle with disturbance uncertainty," *IEEE Transactions on Industrial Electronics*, vol. 62, no. 3, pp. 1563-1571, 2015.

[4] J. Xiong and E. Zheng, "Position and attitude tracking control for a quadrotor UAV," *ISA Transactions*, vol. 53, no. 3, 2014.

[5] C. Tan, J. Wang, Y. Paw and F. Liao, "Autonomous ship deck landing of a quadrotor using invariant ellipsoid method," *IEEE Transactions on Aerospace & Electronic Systems*, vol. 52, no. 2, 2016.

[6] H. Shin, D. You and D. H. Shim, "Autonomous shipboard landing algorithm for unmanned helicopters in crosswind," *Journal of Intelligent & Robotic Systems*, vol. 74, no. 1-2, pp. 347-361, 2013.

[7] R. Lungu and M. Lungu, "Design of automatic landing systems using the H-inf control and the dynamic inversion," *Journal of Dynamic Systems Measurement & Control*, vol. 183, no. 2, 2015.

[8] Z. Liu, Y. Wang and X. Hao, "Coordinated landing control of unmanned aerial vehicle," *International Conference on Electronics, Communications and Contro*, 2011:1965-1970.

[9] S. R. Oh, K. Pathak, S. K. Agrawal, H. R. Pota and M. Garratt, "Approaches for a tether-guided landing of an autonomous helicopter," *IEEE Transactions on Robotics*, vol. 22, no. 3, pp. 536-544, 2006.

[10] Z. Ma, T. Hu and L. Shen, "Stereo vision guiding for the autonomous landing of fixed-wing UAVs: a saliencyinspired approach," *International Journal of Advanced Robotic Systems*, vol.13, 2016.

[11] S. Saripalli and G. S. Sukhatme, "Landing on a moving target using an autonomous helicopter," *Advanced Robotics*, vol. 24, pp. 277-286, 2004.

[12] J. Ghommam and M. Saad, "Autonomous landing of a quadrotor on a moving platform," *IEEE Transactions on Aerospace and Electronic Systems*, 2017, available online.

[13] J. W. Kim, Y. D. Jung, D. S. Lee, and D. H. Shim, "Landing control on a mobile platform for multi-copters using an omnidirectional image sensor," *Journal of Intelligent & Robotic Systems Theory & Applications*, vol. 84, pp. 1-13, 2016.

[14] R. Lungu and M. Lungu, "Application of H_2/H_∞ and dynamic inversion techniques to aircraft landing control," *Aerospace Science & Technology*, vol. 46, pp. 146-158, 2015.

[15] Y. Deng, H. Duan, "Control parameter design for automatic carrier landing system via pigeon-inspired optimization," *Nonlinear Dynamics*, vol. 85, no. 1, pp. 97-106, 2016.

[16] L. Sun and W. Huo, "Robust adaptive relative position tracking and attitude synchronization for spacecraft rendezvous," *Aerospace Science & Technology*, vol. 41, pp. 28-35, 2015.

[17] L. Sun and W. Huo, "Robust adaptive control of spacecraft proximity maneuvers under dynamic coupling and uncertainty," *Advances in Space Research*, vol. 56, no. 10, pp. 2206-2217, 2015.

[18] J. R. Azinheira and A. Moutinho, "Hover control of an UAV with backstepping design including input saturations," *IEEE Transactions on Control Systems Technology*, vol. 16, no. 3, pp. 517-526, 2008.

[19] D. Huang, J. Zhai, W. Ai and S. Fei, "Disturbance observer-based robust control for trajectory tracking of wheeledmobile robots," *Neurocomputing*, pp. 74-79 2016.

[20] F. Chen, R. Jiang, K. Zhang, B. Jiang, and G. Tao, "Robust backstepping sliding mode control and observer-based fault estimation for a quadrotor UAV," *IEEE Transactions on Industrial Electronics*, vol. 63, no. 8, 2016.

[21] Y. Ma, X. Jia, Y. Yan and D. Liu, "Observer-based H_∞ control for nonlinear Markovian jump systems with time-delay and input saturation," *Computational & Applied Mathematics*, pp. 1-21, 2016.

[22] C. Jin, M. Zhu, L. Sun and Z. Zheng, "Relative motion modeling and control for a quadrotor landing on an unmanned vessel," *AIAA Guidance, Navigation, and Control Conference*, AIAA-2017-1522, 2017.

[23] M. Tarek and B. Abdelaziz, "Backstepping control for a quadrotor helicopter," *IEEE/RSJ International Conference on Intelligent Robots and Systems*, pp. 3255-3260, 2006.

[24] P. Mu, "Research on control algorithm of trajectory tracking for unmanned surface vehicle," *Harbin Engineering University, master dissertation*, 2013.

[25] W. Chen, "Disturbance observer based control for nonlinear systems," *IEEE/ASME Transactions on Mechatronics*, pp. 706-710, 2004.

[26] Hassan K. Khalil, "Nonlinear systems, third edition," *Pearson Education, Inc.*, 2012.

[27] R. Skjetne, O. Smogeli and T. Fossen. "A nonlinear ship maneuvering model:identification and adaptive control with experiments," *Modeling Identification & Control*, vol. 25, no. 1, pp. 3-27, 2004.

[28] T. Dierks and S. Jagannathan. "Output feedback control of a quadrotor UAV using neural networks," *IEEE Transactions on Neural Networks*, vol. 21, no. 1, pp. 50-66, 2010.